Available online at www.sciencedirect.com
SCIENCE DIRECT®
ELSEVIER
Journal of Magnetism and Magnetic Materials 293 (2005) 584–588
Journal of magnetism and magnetic materials
www.elsevier.com/locate/jmmm

Magnetic particle diverter in an integrated microfluidic format

Nikola Pekas[a], Michael Granger[a], Mark Tondra[b], Anthony Popple[b], Marc D. Porter[a,*]

[a]*Institute for Combinatorial Discovery, Departments of Chemistry and Chemical Engineering, and Ames Laboratory—USDOE, Iowa State University, Ames, IA 50011-3111, USA*
[b]*NVE Corporation, Eden Prairie, Minnesota 55344, USA*

Available online 3 March 2005

Abstract

A fully integrated micromagnetic particle diverter and microfluidic system are described. Particles are diverted via an external uniform magnetic field perturbed at the microscale by underlying current straps. The resulting magnetic force deflects particles across a flow stream into one of the two channels at a Y-shaped junction. The basic theoretical framework, design, and operational demonstration of the device are presented.

Keywords: Micromagnetic system; Microfluidics; Lab-on-a-chip; Diverter; Flow; Y-shaped junction; Magnetic separation

Magnetic particles coupled to biorecognition agents, such as antibodies or oligonucleotides, are widely used for cell and organelle separation, DNA and protein isolation and purification, and drug screening [1–4]. In these applications, the particle–target complex is retained by the field of an external permanent magnet in order to separate the target from the sample. Magnetic tagging also potentially provides a means to capture, sort, mix, and direct particles in a variety of lab-on-a-chip devices without the use of mechanical parts, such as valves. To realize this goal, however, it is necessary to generate and dynamically control the magnetic field profiles at a micrometer length scale by using, for example, microfabricated electromagnets.

Several microelectromagnet-based, particle-actuation strategies have been reported [5–11]. In some cases, superparamagnetic particles were simply attracted toward a field maximum that was induced by a microelectromagnet in either non-flowing [5,6] or flowing [7,8] suspensions. In previous work [9], we employed a secondary uniform magnetic field to magnetize particles, allowing each microelectromagnetic element to either attract or repel particles, depending on

*Corresponding author. Department of Chemistry, Iowa State University, 42 Spedding Hall, Ames, IA 50010, USA. Tel.: +1 515 294 6433; fax: +1 515 294 3254.
E-mail address: mporter@porter1.ameslab.gov (M.D. Porter).

0304-8853/$ - see front matter © 2005 Published by Elsevier B.V.
doi:10.1016/j.jmmm.2005.01.077

current polarity. Although we demonstrated particle manipulation at the micrometer scale, fluidic integration challenges limited operation to a non-flowing suspension. Other groups exploited a similar approach in order to manipulate particles in non-flowing suspensions at the 100-μm [10] and millimeter [11] scale.

In this report, we describe the first micromagnetic–microfluidic hybrid structure that exerts both attractive and repulsive forces at the micrometer size scale. The design and fabrication, theoretical assessment, and functional demonstration of the rapid and effective diversion of magnetic entities within a fluid stream are presented.

The magnetic force acting on a particle in a magnetic field is proportional to both the particle magnetic moment and the field gradient. The magnetic moment, in turn, is determined by the magnetic field strength and the intrinsic properties of the particle. In our system, a uniform external magnetic field magnetizes the particles, while microfabricated current lines induce a localized field perturbation. As a result, gradients of 10^2–10^3 T/m are generated. Fig. 1 provides further details.

Device fabrication began with the deposition of a 200-nm silicon nitride passivation layer onto a silicon wafer. Next, 1.7-μm thick aluminum current lines were sputter-deposited and etched using reactive ion etching (RIE) and a photoresist etch mask. After etching, the structure was coated with a planarizing layer of benzocyclobuthene (BCB), which had a thickness of 1.8 μm with respect to the top of the aluminum lines. A second BCB layer was then spun to a 6-μm thickness, and etched to form 18-μm wide fluidic channels positioned directly over the current lines. The second BCB layer was coated with 200 nm of silicon nitride to facilitate bonding to a 2-mm thick rectangular slab of poly(dimethylsiloxane) (PDMS) rubber. This step defined the top of the fluidic channels, and added through-channels for external access to the device. The slabs were made by casting a PDMS prepolymer mixture against a polished silicon wafer. Fluidic connections through the slabs were formed by using sacrificial L-shaped inserts affixed to the wafer prior to molding. After curing the PDMS, the inserts were removed and PDMS slab was peeled off the wafer. Both the slabs and silicon nitride-coated devices were activated in oxygen plasma and then aligned and brought into contact using a mask aligner to seal the slab to the device. Finally, the devices were wire-bonded onto printed-circuit boards and tested for electrical and fluidic integrity.

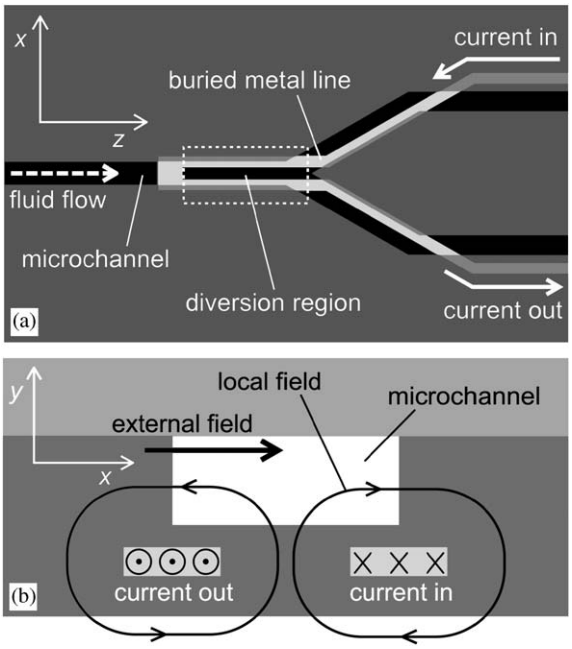

Fig. 1. A micromagnetofluidic diverter: (a) top view and (b) end view schematics. Before the flow-splitting junction, the suspension of magnetic particles flows along the z-axis. Magnetic particles in the flow stream are magnetized by an external magnetic field aligned along the x-axis. The current-carrying metal straps induce a local gradient field that is superimposed on the external field. The magnetic force, which is proportional to the particle magnetization and to the field gradient, deflects the particles away from the field minimum and toward the field maximum. As a consequence, the particles are driven across the flow stream along the x-axis and diverted into a desired channel.

A finished device, mounted on a plastic holder, is shown in Fig. 2. The external field, oriented along the x-axis direction, was applied by placing two miniature rare-earth magnets immediately adjacent to the holder sides. The field uniformity and strength were characterized with the

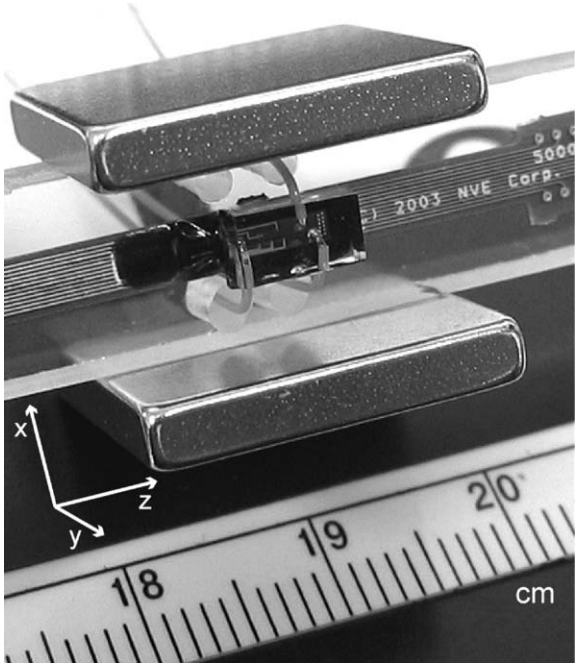

Fig. 2. A micromagnetofluidic device with complete electrical and fluidic connections, mounted on a plastic holder. Fluidic lines (polymeric capillary tubing) are connected to the device through fluidic-access ports located in the sides of the transparent PDMS lid. The device is wire-bonded to a flexible printed-circuit board, and contacts are the potted with a non-conductive epoxy resin. An external magnetic field along the x-axis direction is applied by sandwiching the device between the two miniature square-shaped permanent magnets.

gauss-meter probe that was attached to a micro-manipulator. We positioned the magnets relative to the device so that the field magnitude equaled 16.0 mT, with the variation of 0.6 mT/mm along the z-axis and 0.3 mT/mm along the x-axis. The expected gradients induced by the current straps were at least three orders of magnitude larger than the measured variation in the external field.

To assess performance for a set of experimental parameters, we first modeled the diverter via the following analysis. In a dilute aqueous suspension, the magnetic force $\mathbf{F}_{\text{mag}}$ acting on a superparamagnetic particle in a magnetic field of a free-air inductance $\mathbf{B}$ is given in SI units as [12,13]

$$\mathbf{F}_{\text{mag}} = \frac{V\chi}{\mu_0}(\mathbf{B}\cdot\nabla)\mathbf{B}, \tag{1}$$

where V is the particle volume, χ is the magnetic susceptibility of the particle, and μ_0 is the magnetic permeability in vacuum. Since the current density $\mathbf{J}$ within the microchannel equals zero, Ampère's law ($\nabla\times\mathbf{B}=\mu_0\mathbf{J}$) indicates that the curl of vector $\mathbf{B}$ vanishes within the volume element defined by the microfluidic channel. We can therefore use the identity $\nabla(\mathbf{B}\cdot\mathbf{B}) = 2\mathbf{B}\times(\nabla\times\mathbf{B}) + 2(\mathbf{B}\cdot\nabla)\mathbf{B}$ to transform Eq. (1) into the following:

$$\mathbf{F}_{\text{mag}} = \frac{V\chi}{2\mu_0}\nabla B^2. \tag{2}$$

The magnetic force acting on the particle can now be calculated using Eq. (2). Because of the diverter geometry (long and narrow buried current straps), we can reduce the problem to two dimensions. Thus, the field at any point in the channel cross-section (x–y plane) can be calculated as a sum of the external field and the current-induced contributions determined from the Biot–Savart law. The modeling results, obtained using in-house code written in MATLAB®, are shown in Fig. 3. An extrapolation of the data provided by the vendor for similar particles yielded a χ of about 0.1, which was used in the calculations. In order for the diverter to work effectively, the direction and magnitude of the magnetically derived force on the particle must be relatively uniform. That is, the width and the position of the channel must be designed relative to the current lines in such a way that particles experience only the field flanked by the two straps.

A particle trajectory in the x–y plane can be deduced from the equation of motion involving a viscous-drag force and a magnetic force:

$$m\frac{\mathrm{d}\mathbf{v}}{\mathrm{d}t} = -3\pi\eta a\mathbf{v} + \mathbf{F}_{\text{mag}}, \tag{3}$$

where m is the mass of a particle, $\mathbf{v}$ is the particle velocity across the flow stream, a is the particle diameter, and η is the dynamic viscosity of the carrier fluid ($\eta = 0.890$ mPa s at room temperature [14]). To examine the behavior of a particle, we will assume that $\mathbf{F}_{\text{mag}}$ is a constant perpendicular to the z-axis. The particle will then accelerate along the direction of the force, and the velocity dependence on time is obtained

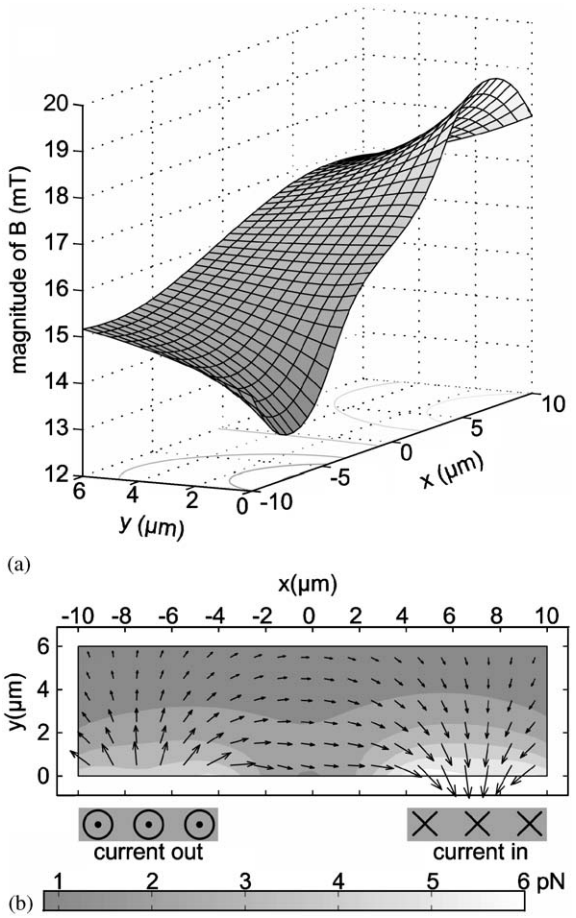

Fig. 3. The magnetic-field and force modeling results, based on a current of 50 mA, 16-mT external uniform field applied along the positive x-axis direction, a particle susceptibility of 0.1, and a particle diameter of 1 μm. (a) The total magnitude of the magnetic field, calculated as a sum of the external field and the current-induced local field. The resultant magnetic force (b), which follows the steepest field gradient.

from Eq. (3):

$$v(t) = \frac{F_{\mathrm{mag}}}{3\pi\eta a}\left(1 - \exp\left(-\frac{3\pi\eta a}{m}t\right)\right). \tag{4}$$

The results (based on a particle diameter of 1 μm, and particle density of 1.4 g/cm^3) show the following: (1) the diverting force acting on a particle is in the order of several piconewtons. (2) According to Eq. (4), the terminal velocity is in the order of several hundreds of micrometers per second, and the particle reaches 90% of its terminal across-the-flow velocity in only about 180 ns. This result indicates that the particle trajectory will closely follow the force field shown in Fig. 3 at the force and length scale of our system. (3) A particle is diverted to the desired channel when magnetic force drags the particle across the channel for up to one-half of the channel width. Since our present design has a 100-μm long diverter region with 18-μm wide channels, the maximum flow velocity is about 3 mm/s.

To visualize the flow of the fluorescent superparamagnetic beads (Bangs Labs 4962, 28% magnetite, 0.96 μm nominal diameter, internally labeled with the Dragon Green dye), we used an epifluorescence microscope equipped with a CCD camera. A dilute aqueous suspension of magnetic beads (5.3×10^6 beads per cm^3, which corresponds to a volume fraction of 2.8×10^{-6}) was pumped from a pressurized vial, with the pumping pressure of 0.1–0.3 bar. The volume flow rate and the consequent bead velocities were held at ~6 nL/min and ~1 mm/s, respectively. A 50-mA current was sourced through the diverter current lines, and images were collected at the rate of one frame per second, with an exposure time of 28 ms per frame. The collected snapshots were processed using Metamorph software by merging the stack of the snapshots into a "see-through" plane in order to present the data in a single image.

A set of first results is presented in Fig. 4. The beads, originally distributed evenly, were directed into the desired channel after the junction, as dictated by the current polarity. We can define the diversion effectiveness function, ε, as $\varepsilon = (p-q)/(p+q)$, where p and q are the respective numbers of beads detected in the desired and undesired channel after the junction. When all the particles are successfully diverted, ε equals 1. When the diverter is inactive, i.e. no current is sourced, p and q will be equal and ε equals zero. For the data in Fig. 4, ε is found to be 0.71. This value corresponds to 85% of the beads flowing down the desired channel, compared to 50% when the diverter was inactive.

We attribute the less-than-100% effectiveness to either one or both of the following factors. First, the actual channel width was 18 μm instead of the

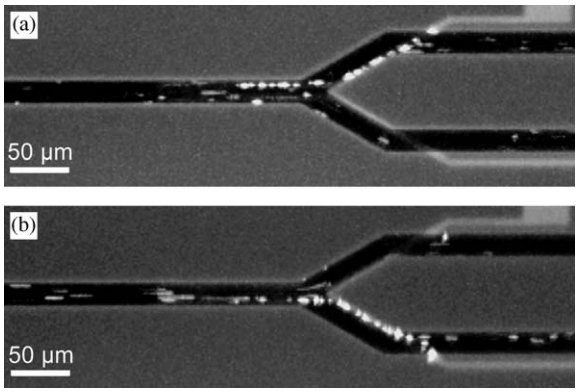

Fig. 4. (a) Fluorescence microphotograph of the diversion region and the flow-splitting junction. The suspension of fluorescent superparamagnetic beads is pumped down the microchannel in the positive z-axis direction. The image is a composite "see-through" plane of 60 individual snapshots collected at a 1 Hz frame rate. Immediately before the flow-splitting junction, particles flow through the 100-μm long magnetic-diverter arena (buried current lines not visible) and are deflected to the upper channel. In (b) the current polarity is inversed, and particles are consequently directed into the lower channel.

targeted 12 μm due to an overetched BCB layer. Because of a larger width, the magnetic beads flowing close to one of the walls may experience a portion of the field where the force direction is opposite to that of the desired one (see Fig. 2). Second, the distribution of the bead sizes was relatively broad, and combining Eqs. (2) and (4) shows that the magnetophoretic velocity of a bead scales with the bead cross-section. Although quantitative data was not available, it is likely that a certain fraction of beads were insufficiently large to realize effective diversion.

In summary, we have demonstrated the valveless, micromagnetic diversion of particles in the flowing stream. Our system is the first reported micromagnetofluidic structure that exerts both attractive and repulsive forces at the micrometer scale. Potential applications are in the area of biomolecule and bioparticle manipulation within microfluidic networks for lab-on-a-chip combinatorial analysis and synthesis. More complex actuation tasks and massively parallel, integrated design are possible and practical by drawing on microfabrication technology already in place.

This work was supported by grants from the NSF and from the DARPA BioMagnetICs program and by the Institute for Combinatorial Discovery of Iowa State University. The Ames Laboratory is operated for the US Department of Energy by Iowa State University under Contract no. W-7405-eng-82.

References

[1] A.B. Kantor, I. Gibbons, S. Miltenyi, et al., in: D. Rectenwald, A. Radbruch (Eds.), Cell Separation Methods and Applications, Marcel Dekker, New York, 1998.
[2] M.D. Fisher, S.C. Frost, Anal. Biochem. 251 (1997) 125.
[3] E. Racila, D. Euhus, A.J. Weiss, et al., Proc. Natl. Acad. Sci. USA 95 (1998) 4589.
[4] G.P. Hatch, R.E. Stelter, J. Magn. Magn. Mater. 225 (2001) 262.
[5] C.S. Lee, R.M. Westervelt, Appl. Phys. Lett. 79 (2001) 3308.
[6] D.L. Graham, H. Ferreira, J. Bernardo, et al., J. Appl. Phys. 91 (2002) 7786.
[7] J.-W. Choi, K.W. Oh, A. Han, et al., Biomed. Microdevices 3 (2001) 191.
[8] H. Suzuki, C.-M. Ho, IEEE Proc. Int. Conf. MEMS 40 (2002).
[9] M. Tondra, et al., IEEE Trans. Magn. 37 (2001) 2621.
[10] T. Deng, et al., Appl. Phys. Lett. 78 (2001) 1775.
[11] A. Rida, V. Fernandez, M.A.M. Gijs, Appl. Phys. Lett. 83 (2003) 2396.
[12] M. Zborowski, et al., J. Magn. Magn. Mater. 194 (1999) 224.
[13] R. Gerber, R.R. Birss, High Gradient Magnetic Separation, Research Studies Press, Chichester, 1983.
[14] D.R. Lide (Ed.), CRC Handbook of Chemistry and Physics, 75th ed., CRC Press, Boca Raton, 1994.